Molecular Therapy
Methods & Clinical Development
Original Article

A Sendai Virus-Based Cytoplasmic RNA Vector as a Novel Platform for Long-Term Expression of MicroRNAs

Masayuki Sano,[1] Asako Nakasu,[1] Manami Ohtaka,[1] and Mahito Nakanishi[1]

[1]Biotechnology Research Institute for Drug Discovery, National Institute of Advanced Industrial Science and Technology (AIST), Central 5, 1-1-1 Higashi, Tsukuba, Ibaraki 305-8565, Japan

Cytoplasmic RNA virus-derived vectors have emerged as attractive vehicles for microRNA (miRNA) delivery as they possess no potential risk of chromosomal insertion. However, their relatively short-term expression limits their use in biological applications that require long-term miRNA manipulation, such as somatic cell reprogramming. Here, we show that a cytoplasmic RNA virus vector based on a replication-defective and persistent Sendai virus (SeVdp) serves as an effective platform for long-term production of miRNAs capable of inducing sequence-specific target suppression. The SeVdp vector was able to simultaneously deliver embryonic stem cell-enriched miRNAs, as well as multiple transcription factors, into fibroblasts, resulting in effective reprogramming into induced pluripotent stem cells. Furthermore, we report that the murine miR-367 hairpin produced elevated levels of mature miRNA when it was incorporated into the SeVdp vector and served as an effective backbone for production of artificial miRNAs. These SeVdp vector-derived artificial miRNAs efficiently inhibited expression of target genes. Our findings provide novel insights into a powerful tool for long-term and targeted gene silencing in areas such as regenerative medicine, gene therapy, and cell therapy.

INTRODUCTION

Small regulatory RNAs, such as small interfering RNAs (siRNAs) and microRNAs (miRNAs), are ~22-nucleotide (nt)-long non-coding RNAs that regulate gene expression in eukaryotic cells at a post-transcriptional level.[1] siRNAs are generated from exogenously delivered double-stranded RNAs (dsRNAs) or short hairpin RNAs (shRNAs), and induce sequence-specific degradation of homologous mRNAs through a process termed RNAi.[2] RNAi-based techniques are widely used for loss-of-function studies, as well as therapeutic applications.[3] By contrast, miRNAs are endogenous small RNAs that enable the fine-tuning of gene expression.[4] Because dysregulation of miRNAs often results in disease onset and progression, miRNA-based therapeutics have been validated in clinical applications for the treatment of cancers, infectious diseases, and heart failure.[5] Additionally, miRNAs have gathered substantial attention as potent modulators of somatic cell reprogramming.[6] Several miRNAs exhibit unique expression profiles in specific cells or tissues, playing important roles in maintaining cell identity.[7] For example, manipulation of cell-specific miRNAs enables conversion of fibroblasts into induced pluripotent stem cells (iPSCs), neurons, or cardiomyocytes,[8–10] potentially facilitating cell therapy and regenerative medicine.

Although dsRNA and shRNA are directly cleaved in the cytoplasm to siRNA by Dicer, a member of the RNase III family, miRNAs are generated through two sequential maturation steps.[11] Initially, miRNA-encoding genes are transcribed as primary miRNAs (pri-miRNAs) by RNA polymerase II (Pol II) in the nucleus; then, an RNase III enzyme, Drosha, and its co-factor DiGeorge syndrome critical region 8 (DGCR8) recognize a stem-loop structure within the pri-miRNA, and process the pri-miRNA to a ~70-nt precursor miRNA (pre-miRNA). Pre-miRNAs are transported to the cytoplasm by exportin-5 and are then cleaved by Dicer to ~22-nt miRNA duplexes. One strand of the duplex associates with an RNA-induced silencing complex (RISC), and then guides the RISC to complementary sequences at the 3′ untranslated region (3′ UTR) of mRNAs.[4] In mammals, most miRNAs bind to a target sequence with imperfect complementarity, resulting in RISC-mediated translational repression and/or mRNA degradation.[12] By contrast, miRNAs can induce RISC-mediated RNA cleavage when bound to the target with perfect complementarity.[13] Notably, the original miRNA sequence within the miRNA stem-loop can be replaced by sequences complementary to any gene of interest, and the resultant small RNA, referred to as an artificial miRNA (amiRNA), triggers potent gene silencing akin to siRNA.[14–16] The amiRNA-based approach was shown to be less cytotoxic than conventional shRNA,[17–19] opening the possibility for therapeutic applications.

To successfully manipulate cellular functions through downregulation of targets by means of small RNAs, efficient delivery systems are required. Although transfection of synthetic siRNA or miRNA

Received 6 February 2019; accepted 24 October 2019;
https://doi.org/10.1016/j.omtm.2019.10.012.

Correspondence: Masayuki Sano, Biotechnology Research Institute for Drug Discovery, National Institute of Advanced Industrial Science and Technology (AIST), Central 5, 1-1-1 Higashi, Tsukuba, Ibaraki 305-8565, Japan.
E-mail: m.sano@aist.go.jp

is relatively easy and safe, virus-mediated transduction has additional advantages, such as high transduction efficiency, broad tropism, and durable expression.[20] Currently, several DNA viral- and integrating viral-vectors serve as common platforms for small RNA delivery.[20] In particular, integrating viral vectors based on retrovirus or lentivirus enable prolonged expression of small RNAs via chromosomal insertion; thus, they are often used as the primary choice when long-term supplementation of small RNAs is required. However, integrating vectors can potentially lead to random insertional mutagenesis, conferring the risk of tumorigenesis in clinical applications.[21] Moreover, gene expression driven by DNA viral promoters or mammalian promoters varies considerably depending on genomic context and epigenetic control, leading to significantly reduced gene expression during long-term manipulation.[22,23]

To overcome these problems, RNA virus-based vectors have emerged as an attractive tool for small RNA delivery.[24–28] In particular, cytoplasmic RNA viruses allow gene expression to be independent of the host transcriptional machinery, and moreover, they have no DNA intermediate phase and do not require nuclear entry as part of their life cycle, thus avoiding the risk of chromosomal insertion. Previous reports have suggested that cytoplasmic RNA virus-delivered pri-miRNAs can be processed into mature miRNAs through non-canonical miRNA biogenesis, providing sequence-specific inhibition of target gene expression.[29] Positive- and negative-strand cytoplasmic RNA viruses, including flavivirus,[24] Sindbis virus,[25] and vesicular stomatitis virus,[27] have been engineered as platforms for miRNA delivery. Although the ensuing miRNA expression in the acute phase of infection was generally robust, it was also relatively short-term.[30] This inherently transient nature limits the applicability of cytoplasmic RNA virus vectors in areas such as somatic cell reprogramming, which require durable transgene expression.[31]

In the present study, we demonstrate that a Sendai virus (SeV)-based vector can serve as an effective platform for small RNA delivery. SeV is a cytoplasmic RNA virus from the *Paramyxovirinae* subfamily that can infect a broad range of animal cells. Importantly, though, it is neither pathogenic nor carcinogenic in humans. Thus far, various applications have been explored to employ an SeV-based vector in medical research and clinical trials.[32] Previously, we developed a unique SeV vector based on a noncytopathic variant of SeV strain Cl.151, referred to as a replication-defective and persistent SeV (SeVdp) vector.[33] The SeVdp vector was shown to stably and persistently express protein-coding genes without chromosomal insertion; however, its potential for small RNA delivery remained elusive. Here, we show that the SeVdp vector serves as a platform for long-term production of functional miRNAs. Moreover, an SeVdp vector expressing embryonic stem cell (ESC)-enriched miRNAs can be applied in somatic cell reprogramming. Furthermore, the murine miR-367 hairpin resulted in a robust level of mature miR-367 when incorporated into the SeVdp vector and, therefore, provided an effective backbone for the production of amiRNAs in the SeVdp vector. Our findings describe a potent new tool for small RNA delivery that enables the effective regulation of gene expression and manipulation of cellular functions.

RESULTS

The SeVdp Vector as an Effective Platform for Long-Term Production of miRNAs

Previous studies suggested that cytoplasmic RNA viruses, Sindbis virus, and vesicular stomatitis virus harboring the murine miR-124-2 (mmu-miR-124-2) locus were able to produce a mature miR-124.[25,27] To examine whether SeV can be engineered to produce miRNAs, we constructed the SeVdp-124 vector containing an approximately 600-bp sequence corresponding to the mmu-miR-124-2 locus (Figure 1A). Transgenes flanked by start and end signals within the SeV RNA genome are transcribed as mRNAs by a viral RNA-dependent RNA polymerase (RdRp). Thus, the mmu-miR-124-2 sequence located between these signals can be synthesized as pri-miR-124 with the 5′ methylated cap and 3′ poly(A) sequence (Figure S1A). The SeVdp-124 vector also contained genes for blasticidin S deaminase (*Bs*^{r}) and *EGFP*, enabling selection and monitoring of infected cells, respectively (Figure 1A).

Human colorectal carcinoma HCT116 cells were infected with SeVdp-124 and then treated with blasticidin S (Bs) to isolate cells stably harboring the SeVdp-124 genome. As a control, HCT116 cells were also infected with the SeVdp-Ctrl vector lacking any miRNA sequence (Figure 1A). To examine whether SeVdp-124 can produce miRNA, we measured the level of mature miR-124 by qRT-PCR. SeVdp-124-infected cells exhibited elevated miR-124 expression compared with that of non-infected and SeVdp-Ctrl-infected cells (Figure S2A). The level of miR-124 in SeVdp-124-infected cells was approximately 20-fold higher than in SeVdp-Ctrl-infected cells (Figure 1B), indicating that the SeVdp vector can produce miR-124 in a similar fashion as reported for other cytoplasmic RNA viruses.[25,27] Importantly, SeVdp-124-infected cells continuously expressed miR-124 and maintained it at a significantly higher level than in SeVdp-Ctrl-infected cells even after 100 days (Figure 1C). These cells also showed durable EGFP expression (Figure S3A), suggesting that the SeVdp vector confers long-term production of miRNA and protein-coding genes.

In addition to SeVdp-124, we constructed SeVdp-9 and SeVdp-302-367, which contained murine genomic loci corresponding to miR-9-3 and miR-302-367, respectively (Figure 1A). Of note, the miR-302-367 locus contained five tandem hairpins for miR-302b, miR-302c, miR-302a, miR-302d, and miR-367, resulting in the production of multiple miRNAs from a single transcript (Figure S1B).[34] HCT116 cells were infected with SeVdp-9 or SeVdp-302-367, and miRNA levels were measured after treating the cells with Bs. Compared with non-infected and SeVdp-Ctrl-infected cells, SeVdp-9-infected cells produced more miR-9 (Figures S2B and S4A). Similarly, SeVdp-302-367-infected cells generated considerably more miR-302a, miR-302b, miR-302c, miR-302d, and miR-367 than those generated by control cells (Figure 1D; Figure S2C), indicating that SeVdp-delivered pri-miRNAs were properly processed into their respective miRNAs. Moreover, we monitored miRNA expression in HeLa cells stably infected with

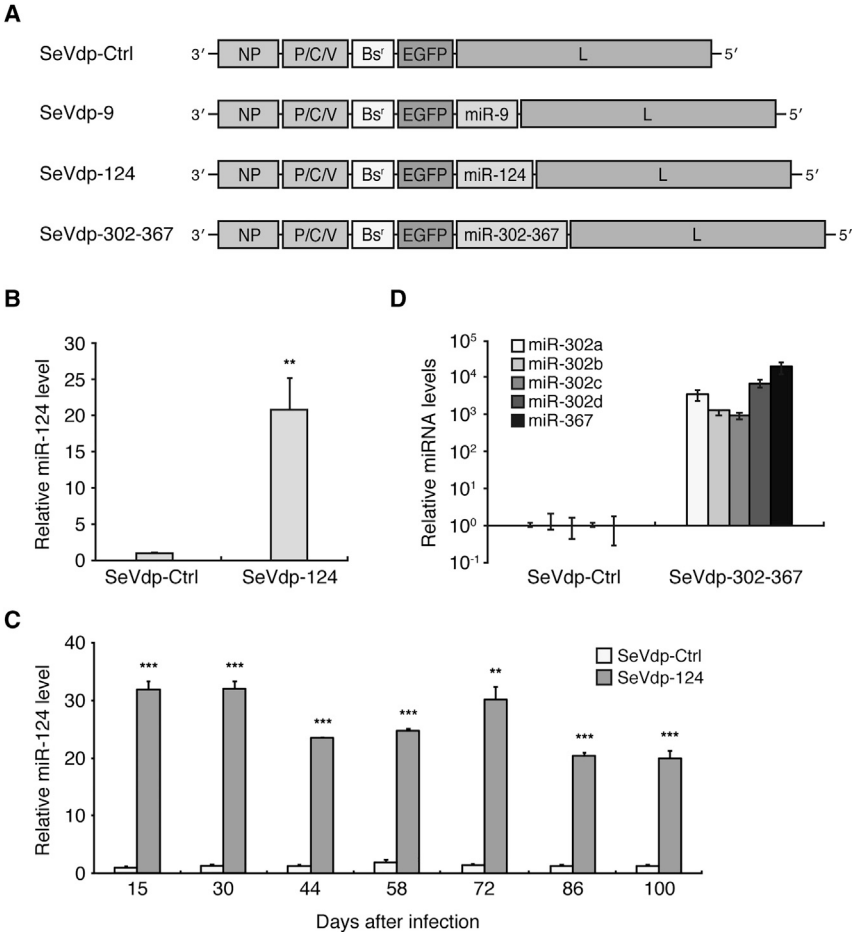

Figure 1. SeVdp Vector-Mediated miRNA Expression

(A) Genome structure of the SeVdp vectors. *NP*, *P*, and *L* genes are indispensable for the replication of the viral genome and mRNA synthesis. The *P* gene contains multiple open reading frames encoding P, C, and V proteins. The SeVdp genome encodes Bs^r, EGFP, and murine miRNA as transgenes. (B) Expression of miR-124 in HCT116 cells infected with either SeVdp-Ctrl or SeVdp-124; miR-124 levels were determined by qRT-PCR; the level in SeVdp-Ctrl-infected cells was set to 1.0. $^{**}p < 0.05$ versus SeVdp-Ctrl. (C) Long-term miRNA expression in HCT116 cells infected with SeVdp-Ctrl or SeVdp-124. Infected cells were continuously cultured in the presence of Bs. miR-124 level in SeVdp-Ctrl-infected cells on day 15 was set to 1.0. $^{**}p < 0.005$, $^{***}p < 0.001$ versus SeVdp-Ctrl on day 15. (D) Expression of miR-302s (miR-302a, miR-302b, miR-302c, and miR-302d) and miR-367 in SeVdp-302-367-infected cells, as determined by qRT-PCR. miRNA levels in SeVdp-Ctrl-infected cells were set to 1.0. Data are presented as the mean ± SD (n = 3).

SeVdp-124, SeVdp-302-367, or SeVdp-9, and found that those cells produced higher levels of corresponding miRNAs than did the cells infected with SeVdp-Ctrl over a long period of time (Figure S3B).

SeVdp Vector-Mediated miRNA Delivery and Target Suppression

As the SeVdp vector can efficiently deliver transgenes into mammalian cells,[33] we sought to examine SeVdp vector-mediated miRNA production in various human cells. Adherent cells including HeLa, HEK293, A549, and normal human dermal fibroblasts (NHDFs), as well as suspension cells such as Jurkat and U937, were infected with SeVdp-Ctrl or SeVdp-124, and then miR-124 levels were measured after treating the cells with Bs. qRT-PCR analysis indicated that all SeVdp-124-infected cells had high levels of miR-124 compared with that of SeVdp-Ctrl-infected cells (Figure 2A). miRNA production was more effective in adherent cells and especially in A549 cells, where it was 45-fold higher than in the corresponding controls. Even though U937 cells expressed considerably more endogenous miR-124 relative to other cell types (Figure S5), SeVdp-124 managed to further increase production of miR-124 in these cells (Figure 2A). These data indicate that the SeVdp vector can deliver miRNAs into various human cells, including suspension cells and primary cells.

We next examined whether an SeVdp vector expressing miRNAs can cause sequence-specific gene suppression. To this end, we constructed psiCHECK reporter plasmids containing firefly and *Renilla* luciferase genes, as well as one copy of a sequence perfectly complementary to the target miRNA and located at the 3′ UTR of the *Renilla* luciferase gene. The psi-124T, psi-302aT, and psi-9T plasmids contained the complementary sequences for miR-124, miR-302a, and miR-9, respectively. The control psi-124scrT, psi-302ascrT, and psi-9scrT plasmids contained the scrambled sequences for each miRNA. In this system, miRNA-mediated target cleavage lowers the expression of *Renilla* but not firefly luciferase. Therefore, the value of *Renilla* versus firefly luciferase activities readily indicates the inhibitory activity of the specific miRNAs. SeVdp-Ctrl-infected and SeVdp-124-infected HCT116 cells were cultured with Bs for 32 days, followed by transfection with psi-124T or psi-124scrT, after which the firefly and *Renilla* luciferase activities were measured. As shown in Figure 2B, luciferase activity was significantly reduced after psi-124T transfection compared with psi-124scrT in SeVdp-124-infected cells but not in SeVdp-Ctrl-infected cells, indicating that SeVdp-124-derived miR-124 inhibited target expression in a sequence-dependent manner. Similarly, the luciferase activity of psi-302aT was decreased in cells stably infected with SeVdp-302-367 but not SeVdp-Ctrl (Figure 2C). We also observed a significant reduction in the luciferase activity of SeVdp-9-infected cells, with endogenous miR-9 dropping to basal levels and corresponding to psi-9T activity (Figure S4B). These findings suggest that the SeVdp vector can be used successfully as a platform for long-term production of functional miRNAs.

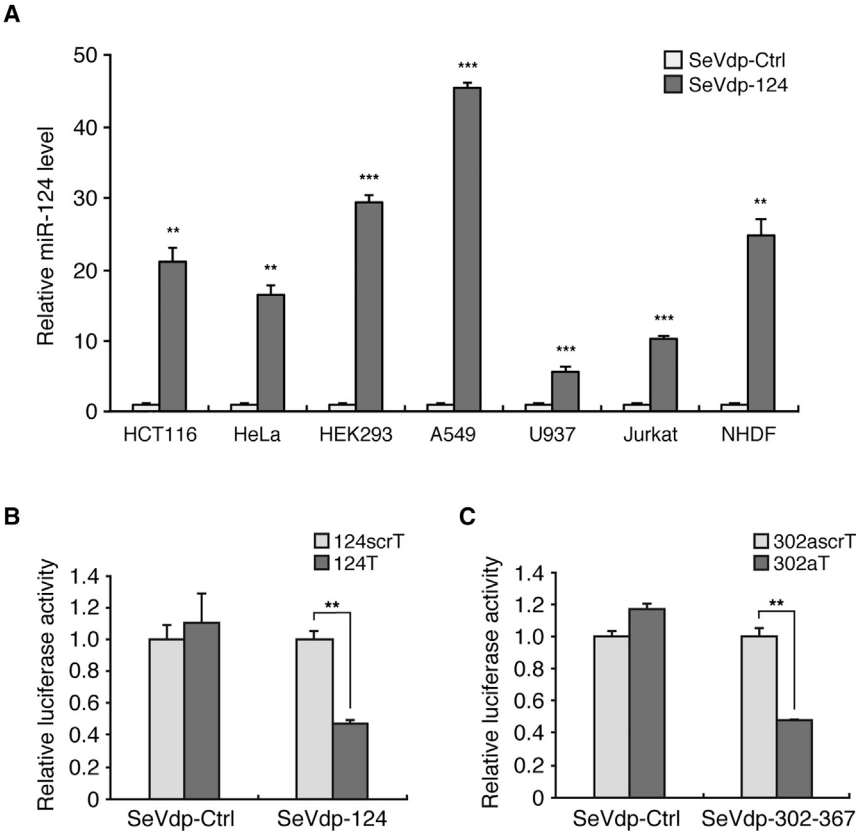

Figure 2. The SeVdp Vector as a Platform for Expressing Functional miRNAs

(A) miRNA expression in various human cells infected with SeVdp-Ctrl or SeVdp-124. miR-124 levels were determined by qRT-PCR; the level in SeVdp-Ctrl-infected cells was set to 1.0. $^{**}p < 0.005$, $^{***}p < 0.001$ versus SeVdp-Ctrl. (B) Inhibitory activity of SeVdp-124 determined in SeVdp-Ctrl- and SeVdp-124-infected cells transfected with psi-124T or psi-124scrT. The ratio of firefly (Fluc) and *Renilla* (Rluc) luciferase activities was determined; the Rluc/Fluc ratio in psi-124scrT-transfected cells was set to 1.0. $^{**}p < 0.001$. (C) Inhibitory activity of SeVdp-302-367 determined in SeVdp-Ctrl- and SeVdp-302-367-infected cells transfected with psi-302aT or psi-302ascrT. The Rluc/Fluc ratio of psi-302ascrT-transfected cells was set to 1.0. Data are presented as the mean ± SD (n = 3). $^{**}p < 0.001$.

Somatic Cell Reprogramming with SeVdp Vectors Expressing ESC-Enriched miRNAs

Several lines of evidence have suggested that manipulation of ESC-enriched miRNAs plays crucial roles in somatic cell reprogramming.[6] In particular, miR-302-367 and miR-200 family members were shown to promote reprogramming when combined with transcription factors such as OCT4, SOX2, and KLF4.[35–37]

To verify the biological applicability of SeVdp vectors capable of prolonged miRNA expression, we tested the efficacy of SeVdp vectors harboring ESC-enriched miRNAs in iPSC generation. We constructed SeVdp(302-367) and SeVdp(200c) vectors containing the mmu-miR-302-367 and mmu-miR-200c loci, respectively (Table S1). Additionally, we prepared the SeVdp(302-367/200c) vector containing both miRNA loci on a single vector backbone and allowing simultaneous expression of miR-302s (miR-302a, miR-302b, miR-302c, and miR-302d), miR-367, and miR-200c. The SeVdp(empty) vector lacking any transgenes was used as a control. These vectors were used to co-infect mouse embryonic fibroblasts (MEFs) with the SeVdp(K/O/S) vector encoding KLF4, OCT4, and SOX2; the number of colonies positive for the pluripotency marker SSEA1 was counted on day 14 after infection. Co-infection of SeVdp(K/O/S) with SeVdp(empty) had a marginal effect on colony formation, suggesting that SeVdp(K/O/S) alone was unable to efficiently reprogram MEFs into miPSCs (Figure 3A). By contrast, co-infection of SeVdp(K/O/S) with SeVdp(302-367) or SeVdp(200c) increased the number of SSEA1+ colonies. Of note, co-infection of SeVdp(302-367/200c) with SeVdp(K/O/S) markedly promoted SSEA1+ colony formation, suggesting that SeVdp vector-derived miRNAs played a role in somatic cell reprogramming.

As the combination of miR-302-367 with miR-200c showed a significant effect in cell reprogramming, we prepared an SeVdp vector that contained miR-302-367, miR-200c, KLF4, OCT4, and SOX2 on a single vector backbone, referred to here as SeVdp(302-367/200c/K/O/S). Single infection with SeVdp(302-367/200c/K/O/S) was expected to improve reprogramming efficiency over separate infections with SeVdp(302-367/200c) and SeVdp(K/O/S) because the single vector enables uniform expression of all the transgenes in individual infected cells.[33] MEFs were infected with SeVdp(302-367/200c/K/O/S), and SSEA1+ colonies were counted 14 days after infection. As expected, SeVdp(302-367/200c/K/O/S) significantly enhanced the generation of SSEA1+ colonies, whereas control SeVdp vectors had no or only a marginal effect (Figure 3B). We confirmed that SeVdp(302-367/200c/K/O/S) simultaneously expressed miR-302a, miR-367, miR-200c, OCT4, SOX2, and KLF4 in SeVdp(302-367/200c/K/O/S)-infected MEFs (Figure S6). These findings indicate that SeVdp vector-derived ESC-enriched miRNAs have a potent effect on induction of somatic cell reprogramming, thereby facilitating iPSC generation.

Previously, we demonstrated that the SeVdp vector can be removed from infected cells by blocking SeV RdRp activity using siRNA.[33] This procedure was successfully applied for the removal of SeVdp vectors from reprogrammed iPSC colonies, resulting in the generation of transgene-free iPSCs.[33] To establish transgene-free miPSCs generated with SeVdp(302-367/200c/K/O/S), the reprogrammed colonies were treated with siRNA against the SeV polymerase *P* or *L* gene (siP234 or siL527), after which colonies were manually picked to

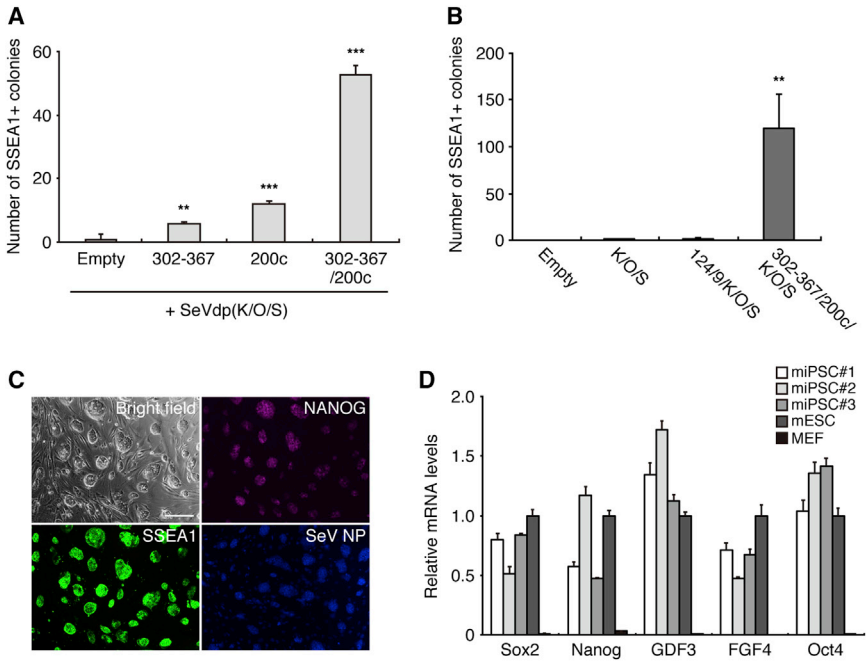

Figure 3. Generation of miPSCs with SeVdp Expressing ESC-Enriched miRNAs

(A) Enhanced miPSC colony formation in MEFs co-infected with SeVdp(K/O/S) and SeVdp expressing ESC-enriched miRNA(s). SSEA1+ colonies were counted on day 14 after infection. **$p < 0.005$, ***$p < 0.001$ versus Empty. Empty, SeVdp(empty); 302-367, SeVdp(302-367); 200c, SeVdp(200c); 302-367/200c, SeVdp(302-367/200c). (B) Generation of miPSCs with a single SeVdp vector expressing miRNAs and reprogramming factors. MEFs were infected with SeVdp(empty), SeVdp(K/O/S), SeVdp(124/9/K/O/S), or SeVdp(302-367/200c/K/O/S), after which SSEA1+ colonies were counted on day 14 after infection. SeVdp(124/9/K/O/S) contains mmu-miR-124-2 and mmu-miR-9-3 loci, as well as the genes for *KLF4*, *OCT4*, and *SOX2* on a single vector backbone. **$p < 0.05$ versus SeVdp(K/O/S). (C) Expression of pluripotency marker proteins SSEA1 and NANOG in miPSC clones (#1) generated with SeVdp(302-367/200c/K/O/S). The clone was also incubated with a primary antibody against the SeV-NP antigen, and nuclei were stained with DAPI. Scale bar, 200 μm. (D) Expression of ESC marker genes in miPSC clones (#1, #2, and #3) generated with SeVdp(302-367/200c/K/O/S) as determined by qRT-PCR. mRNA levels of mESCs were set to 1.0. Data are presented as the mean ± SD (n = 3).

obtain miPSC clones. The clones exhibited a rounded morphology resembling mouse ESCs (mESCs) and expressed the pluripotency markers NANOG and SSEA1 (Figure 3C; Figure S7). qRT-PCR indicated that the clones expressed other pluripotency marker genes, including *Sox2*, *Oct4*, *GDF3*, and *FGF4* (Figure 3D). Importantly, all clones were negative for the SeV-NP antigen (Figure 3C; Figure S7), suggesting that SeVdp(302-367/200c/K/O/S) was effective for somatic cell reprogramming and the establishment of transgene-free miPSCs.

Efficient Expression of miR-367 by SeVdp Vectors

Because SeVdp vectors were shown to express miRNAs efficiently, we next investigated whether SeVdp vectors can be used as a platform for the production of amiRNAs. According to previous reports, miRNA hairpins, such as pre-miR-30 and pre-miR-155, can serve as effective backbones for producing functional amiRNAs when using retroviral and plasmid vectors.[14,15] Efficient processing of the miRNA hairpin requires optimal sequence and structural elements favorably recognized by miRNA processing enzymes such as Drosha.[38–40] Although it is unclear which features are important for non-canonical processing of miRNA hairpins derived from cytoplasmic RNA virus vectors, the choice of a suitable miRNA hairpin is paramount for SeVdp vectors to act as an effective platform for the production of functional amiRNAs. Interestingly, our luciferase assay data revealed that SeVdp-302-367 strongly inhibited the psi-367T plasmid, which contained the complementary sequence for miR-367 (Figure 4A). The extent by which luciferase activity of psi-367T was reduced was considerably higher than that of psi-302aT in SeVdp-302-367-infected cells (see Figure 2C for comparison). Additionally, the inhibitory activity of SeVdp-302-367 against psi-367T was markedly higher compared to that of SeVdp-124 and SeVdp-9 against psi-124T and psi-9T, respectively (compare Figure 4A to Figures 2B and S4B). These results led us to speculate that the miR-367 hairpin may be a favorable substrate for miRNA processing. To evaluate miR-367 expression by SeVdp-302-367, we compared miRNA levels in SeVdp-302-367-infected HCT116 cells with those in human iPSCs (hiPSCs); the latter are known to express abundant ESC-specific miRNAs including miR-302s and miR-367.[41] qRT-PCR indicated that hiPSCs expressed considerably more miR-302s compared with that of SeVdp-302-367-infected HCT116 cells (Figure S8A). Indeed, miR-302a, miR-302b, miR-302c, and miR-302d were approximately 30-, 77-, 116-, and 18-fold more abundant in hiPSCs than in SeVdp-302-367-infected cells, respectively (Figure S8B). By contrast, miR-367 differed by only 3.7-fold, suggesting that SeVdp-302-367 produced substantially more miR-367 than miR-302s.

We further compared miRNA levels in SeVdp-302-367-infected HCT116 cells with those in cells infected with the retroviral CX4 vector containing mmu-miR-302-367, referred to here as CX4-302-367. CX4-302-367-infected cells were cultured with puromycin to obtain stable transformants. We confirmed that the cells harbored 1.37 ± 0.03 copies of provirus DNA within the chromosome. Interestingly, we found that miR-367 levels were ~13.5-fold higher in SeVdp-302-367-infected cells than in CX4-302-367-infected ones (Figure 4B). By contrast, the levels of miR-302b, miR-302c, and miR-302d were comparable between the two cell types, whereas miR-302a levels were slightly higher in SeVdp-302-367-infected cells. The same trend was observed in SeVdp-302-367-infected and CX4-302-367-infected HeLa S3 cells (Figure S9A). SeVdp-302-367-infected HeLa S3 cells exhibited significantly reduced luciferase activity

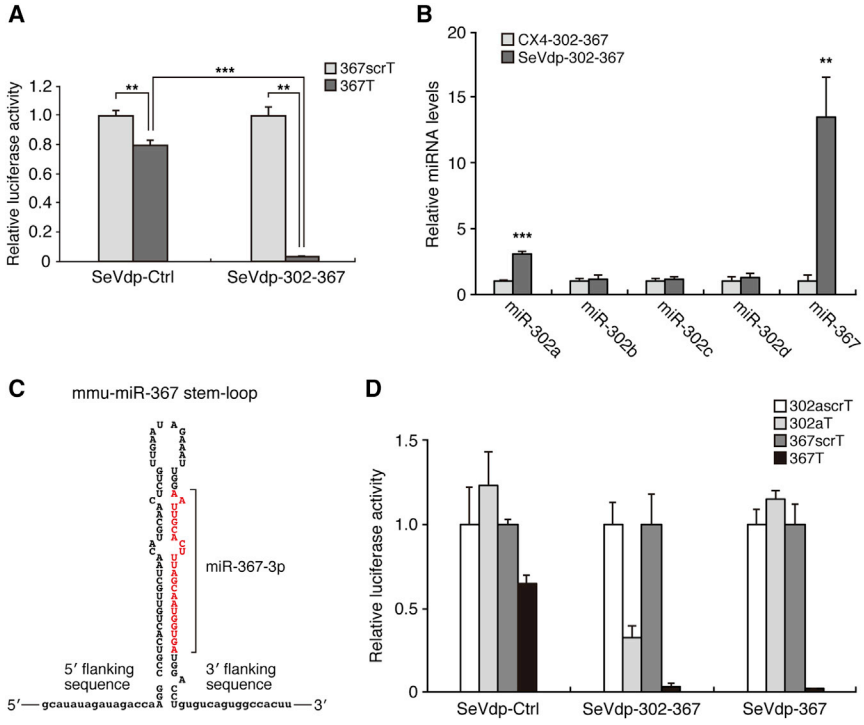

Figure 4. Expression of miR-367 Mediated by the SeVdp Vector

(A) Inhibitory activity of SeVdp-302-367 against the psi-367T vector. SeVdp-Ctrl- and SeVdp-302-367-infected HCT116 cells were transfected with psi-367T or psi-367scrT, and luciferase activities were determined. The Rluc/Fluc ratio of psi-367scrT-transfected cells was set to 1.0. **$p < 0.005$, ***$p < 0.001$. (B) Comparison of miR-302s and miR-367 levels between SeVdp-302-367- and CX4-302-367-infected HCT116 cells. miRNA levels of CX4-302-367-infected cells were set to 1.0. **$p < 0.05$, ***$p < 0.001$ versus CX4-302-367. (C) Structure of the mmu-miR-367 hairpin. The sequence corresponding to miR-367-3p is indicated in red. (D) Inhibitory activity of SeVdp-367 in HCT116 cells infected with SeVdp-Ctrl, SeVdp-302-367, or SeVdp-367 and transfected with the luciferase reporter plasmids. The Rluc/Fluc ratio of psi-302ascrT- and psi-367scrT-transfected cells was set to 1.0. Data are presented as the mean ± SD (n = 3).

with psi-302aT and, particularly, psi-367T (Figures S9B and S9C). These findings suggest that the miR-367 hairpin can be efficiently processed to mature miRNAs when the miR-302-367 cluster is delivered by the SeVdp vector.

To evaluate the efficacy of the miR-367 hairpin, we incorporated the miR-367 stem-loop and the 16-nt 5′ and 3′ natural flanking sequences into the SeVdp vector, yielding SeVdp-367 (Figure 4C). HCT116 cells were infected with SeVdp-367, followed by selection with Bs; the inhibitory activity of the vector was measured by the luciferase assay. Whereas SeVdp-367-infected cells completely lost activity with psi-302aT, the same cells exhibited a significant reduction in luciferase activity with psi-367T (Figure 4D), suggesting that the SeVdp vector-derived miR-367 hairpin can efficiently produce mature miR-367 and thereby increase the inhibitory activity of miRNA.

Efficacy Evaluation of the miR-367 Backbone for amiRNA Production

As the SeVdp vector-derived miR-367 hairpin was effectively processed into miR-367, we attempted to construct an SeVdp vector containing the miR-367 hairpin-based amiRNAs. To this end, the sequence corresponding to miR-367-3p was replaced by the 22-nt sequence complementary to the firefly luciferase gene, and the opposite strand was modified to retain the miR-367 hairpin-like structure in accordance with the secondary structure predicted using the mfold web server (Figure S10).[42] The resultant hairpin was incorporated into the SeVdp vector to yield SeVdp-amiFluc(367) (Table S1). To evaluate the activity of SeVdp-amiFluc(367), we constructed SeVdp vectors containing the complementary sequence for the firefly luciferase gene within the hairpin for mmu-miR-124, has-miR-30, mmu-miR-155, or mmu-miR-302a, yielding SeVdp-amiFluc(124), SeVdp-amiFluc(30), SeVdp-amiFluc(155), or SeVdp-amiFluc(302a), respectively (Figure S10). The hairpins for miR-30, miR-155, and miR-124 were previously shown to efficiently produce amiRNAs by retroviral, plasmid, and Sindbis virus vectors, respectively.[14,15,43] HCT116 cells were infected with either vector, followed by treatment with Bs. All SeVdp-amiFluc-infected cells displayed similar EGFP expression, suggesting that each SeVdp vector expressed comparable levels of transgenes (Figure S11A). To examine amiRNA activity, we co-transfected the SeVdp vector-infected cells with the firefly and *Renilla* luciferase-expression plasmids and determined firefly versus *Renilla* luciferase activities. Although SeVdp-amiFluc(30) and SeVdp-amiFluc(124) effectively inhibited luciferase activity, SeVdp-amiFluc(367) showed greater efficacy (Figure 5A). By contrast, SeVdp-amiFluc(155) and SeVdp-amiFluc(302a) were less effective at inhibiting luciferase expression.

We next examined the activities of the same series of amiRNAs driven by the cytomegalovirus (CMV) immediate-early enhancer/promoter. Plasmid vectors pCMV-amiFluc(367), pCMV-amiFluc(124), pCMV-amiFluc(30), pCMV-amiFluc(155), and pCMV-amiFluc(302a) were prepared and co-transfected with the firefly and *Renilla* luciferase-expression plasmids into HCT116 cells. Although all vectors decreased luciferase activity, pCMV-amiFluc(367), pCMV-amiFluc(124), and pCMV-amiFluc(30) were particularly effective (Figure S11B); activities of these three amiRNAs were nearly identical. Interestingly, we found that pCMV-amiFluc(155) significantly inhibited luciferase expression (Figure S11B) even though SeVdp vector-derived amiFluc(155) showed only marginal activity (Figure 5A). pCMV-amiFluc(302a) also decreased luciferase activity, but the effect was not significant. These data suggest that amiRNAs possessed

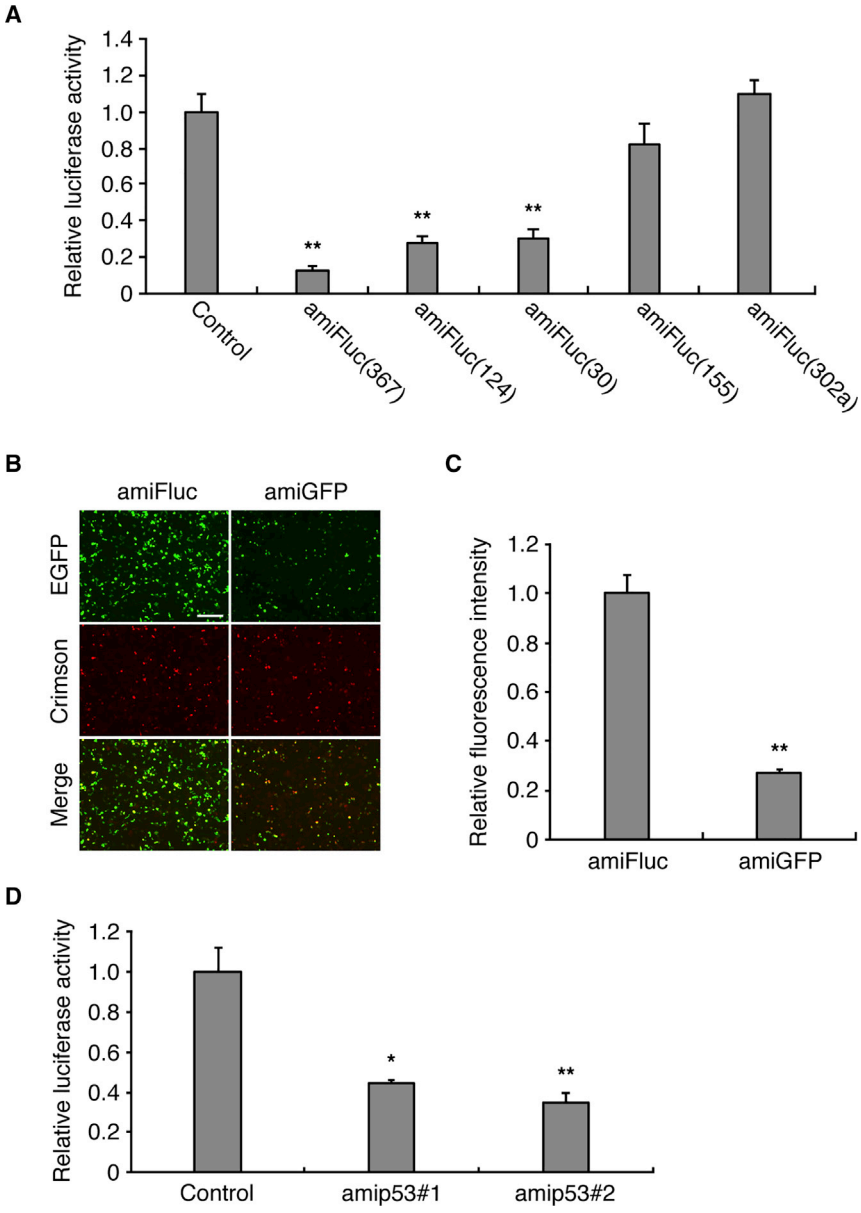

Figure 5. Potency of amiRNA Mediated by SeVdp Vectors

(A) Comparison of the inhibitory activities of amiRNAs with different miRNA backbones in HCT116 cells co-transfected with the firefly and *Renilla* luciferase reporter plasmids. The Fluc/Rluc ratio of SeVdp-Ctrl-infected cells was set to 1.0. **$p < 0.001$ versus control. (B) Inhibitory activity of SeVdp(amiGFP). HCT116 cells were infected with SeVdp(amiFluc) or SeVdp(amiGFP), and co-transfected with EGFP and E2-Crimson expression plasmids. Pseudo-colored images showing EGFP and E2-Crimson expression are shown. Scale bar, 200 μm. (C) Quantitative evaluation of SeVdp(amiGFP) activity. EGFP levels of E2-Crimson+ cells were analyzed by flow cytometry. The mean fluorescence intensity of SeVdp(amiFluc)-infected HCT116 cells was set to 1.0. **$p < 0.001$ versus amiFluc. (D) Inhibitory activity of SeVdp-amip53 in HCT116 cells infected with SeVdp-amip53#1 or SeVdp-amip53#2 and transfected with psi-p53T. The Rluc/Fluc ratio of SeVdp-Ctrl-infected cells was set to 1.0. Data are presented as the mean ± SD (n = 3). *$p < 0.005$, **$p < 0.001$ versus control.

different activity depending on whether they were plasmid- or SeVdp vector-derived, which can be explained by the different modes of miRNA processing between the nucleus and cytoplasm.

Among the pre-miRNA hairpins examined, the mmu-miR-367 backbone was the most effective for amiRNA production by both the plasmid and SeVdp vectors. We also tested the efficacy of the miR-367 hairpin using a different vector backbone, such as lentivirus (LV). We constructed an LV-amiFluc vector containing amiFluc(367) driven by a mouse phosphoglycerate kinase (PGK) promoter, as well as the *EGFP*-fused *Bs*^{r} driven by the simian virus 40 (SV40) promoter in the single vector backbone. EGFP and Bs^r enable monitoring and selection of vector-infected cells, respectively. As a control, the LV vector containing miR-367 instead of amiFluc(367) was prepared. HCT116 cells were infected with LV-367 or LV-amiFluc, followed by treatment with Bs and co-transfection with the firefly and *Renilla* luciferase-expression plasmids. LV-amiFluc-infected cells showed a significant reduction in luciferase activity compared with that of LV-367-infeced cells, indicating that the miR-367 backbone is also effective in the lentiviral vector platform (Figure S11C).

Potency of SeVdp Vector-Driven amiRNAs

To further confirm the efficacy of the miR-367 hairpin in SeVdp vectors, we constructed an SeVdp vector containing the miR-367-based amiRNA targeted against *EGFP* and termed it SeVdp(amiGFP) (Figure S10). The SeVdp(amiGFP) vector also contained genes for *Keima-Red* and hygromycin B phosphotransferase (*Hyg*^{r}), allowing for selection of cells stably harboring the SeVdp(amiGFP) genome (Table S1). SeVdp(amiFluc) containing miR-367-based amiFluc, *Keima-Red*, and *Hyg*^{r} was used as a control. HCT116 cells were infected with SeVdp(amiGFP) or SeVdp(amiFluc), followed by treatment with hygromycin B (Hyg). The infected cells were co-transfected with the EGFP- and E2-Crimson-expression plasmids, and reporter expression was observed by fluorescence microscopy. As shown in Figure 5B, EGFP was significantly reduced in SeVdp(amiGFP)-infected cells compared with SeVdp(amiFluc)-infected cells, whereas E2-Crimson expression was comparable between them. Flow cytometry indicated that the EGFP intensity of SeVdp(amiGFP)-infected cells was 73% lower than that of SeVdp(amiFluc)-infected cells

(Figure 5C), indicating elevated potency of the miR-367 hairpin as a backbone for SeVdp vector-derived amiRNAs.

Next, we designed SeVdp vectors containing miR-367-based amiRNA against two different sites of the murine *p53* gene and termed them SeVdp-amip53#1 and SeVdp-amip53#2 (Figure S10; Table S1). HCT116 cells were infected with SeVdp-amip53 or SeVdp-Ctrl, followed by treatment with Bs and subsequent transfection with the psiCHECK reporter plasmid psi-p53T, which contains the entire coding sequence of the murine p53 located at the 3′ UTR of the *Renilla* luciferase gene. SeVdp-amip53#1- and SeVdp-amip53#2-infected cells showed significantly reduced luciferase activity of psi-p53T (Figure 5D), indicating the potency of SeVdp-amip53. To examine the effect of SeVdp-amip53 on target mRNA expression, we infected mouse NIH 3T3 cells with SeVdp-amip53 and measured *p53* mRNA levels by qRT-PCR after selection with Bs. SeVdp-amip53-infected cells exhibited lower levels of *p53* mRNA compared with that of SeVdp-Ctrl-infected cells (Figure S12A). Luciferase assays using psi-p53T indicated that SeVdp-amip53-infected NIH 3T3 cells had a significant reduction in luciferase activity (Figure S12B), indicating that SeVdp-amip53 can inhibit target expression on both the mRNA and protein level.

DISCUSSION

Here, we demonstrate that the SeVdp vector serves as an effective platform for long-term production of miRNAs. Incorporation of miRNA genes into the SeVdp vector allows synthesis of pri-miRNA transcripts, followed by production of mature miRNAs (Figure 1; Figure S1). Because SeV infects mammalian cells primarily via the ubiquitous sialic acid receptor, the SeVdp vector was able to deliver miRNAs into various human cells (Figure 2A). Of note, SeVdp vectors did not show any apparent cytotoxicity and enabled continuous long-term production of miRNA without any significant loss to its level of expression (Figure 1C). These features are highly advantageous for the delivery of small RNAs in various biological and medical applications.

In addition to remarkable infectivity and durability, we report that the SeVdp vector expressed multiple small non-coding RNAs and protein-coding genes simultaneously (Figure 1C; Figure S3A). Previously, we demonstrated that the SeVdp vector harboring *KLF4*, *OCT4*, *SOX2*, and *c-MYC* efficiently reprogrammed mouse and human somatic cells into iPSCs.[33,44] Notably, subsequent removal of the SeVdp vector from reprogrammed colonies allows the generation of transgene-free iPSCs and the preparation of safer iPSC-derived tissue cells.[45,46] Although the combination of OCT4, SOX2, KLF4, and c-MYC is most frequently used for iPSC generation, c-MYC can be substituted by other factors to reduce the risk of tumor formation.[47] Among known reprogramming factors, ESC-enriched miRNAs, including miR-302-367, miR-372, and miR-200 family, were shown to facilitate cell reprogramming without c-MYC.[35–37,48] Given that a single miRNA can modulate a number of targets simultaneously, miRNAs are powerful tools for manipulating cell fate.[6] For durable miRNA supplementation, chromosomal insertion of miRNA expression cassettes using retroviral or lentiviral vectors or repetitive transfection of synthetic miRNA mimics are often implemented. Although these methods have been commonly used in cell reprogramming, there are crucial concerns such as safety, cost-effectiveness, and transduction efficiency. Additionally, separate introduction of reprogramming factors using these methods may significantly reduce overall reprogramming efficiency.[33] By contrast, the SeVdp vector can accommodate all miRNAs and transcription factors on a single vector backbone and transduce them into cells with a single-round of infection. We showed here that SeVdp(302-367/200c/K/O/S) simultaneously expressed all the genes in transduced cells, resulting in efficient reprogramming of MEFs into iPSCs (Figure 3B; Figure S6). Recent studies have demonstrated that synergistic activities of lineage-specific miRNAs and transcription factors enabled direct conversion of fibroblasts into neurons and cardiomyocytes by bypassing the pluripotent state.[9,10] Thus, it is expected that the SeVdp vector becomes an invaluable cell reprogramming tool capable of producing multiple miRNAs and reprogramming factors.

Our findings demonstrate that SeVdp vectors allow for effective production of amiRNAs. Generally, shRNA driven by a U6 or H1 promoter is used for robust expression of siRNA, resulting in considerable gene silencing.[49] However, shRNA gives rise to severe cytotoxicity through saturation of the endogenous miRNA pathway.[50] By contrast, amiRNAs were shown to be strong RNAi effectors, while significantly attenuating cytotoxicity and the immune response.[17–19] Accordingly, the amiRNA-based approach may provide a more advantageous tool for therapeutic applications. Following the successful use of miR-30 and miR-124 hairpins as backbones for amiRNAs in a cytoplasmic RNA vector based on the Sindbis virus,[43] we showed here that miR-30- and miR-124-based amiRNAs expressed by SeVdp vectors efficiently inhibit expression of the target gene (Figure 5A). Intriguingly, we found that the miR-367-based amiRNA was more effective than miR-30- and miR-124-based amiRNAs when these miRNA hairpins were expressed by SeVdp vectors (Figure 5A). At the opposite end, the miR-302a-based amiRNA was the least effective in target suppression (Figure 5A), suggesting that the processing efficiency of miRNA hairpins strongly affected amiRNA activity. Our findings demonstrate that the miR-367 hairpin is an effective backbone for the production of amiRNAs in SeVdp vectors; accordingly, the miR-367-based approach may improve the efficacy of amiRNAs expressed by other cytoplasmic RNA virus vectors.

Although most miRNAs are generated by canonical miRNA biogenesis including stepwise maturations in the nucleus and cytoplasm, many non-canonical miRNA biogenesis modes that bypass at least one event of the canonical pathway have been identified.[51] As cytoplasmic RNA virus-derived pri-miRNAs are unlikely to encounter Drosha and DGCR8 in the nucleus, they should undergo pri-miRNA processing in the cytoplasm.[29] It was suggested that pri-miRNA transcripts can be processed by Drosha in the cytoplasm because nuclear Drosha relocates to the cytoplasm after infection with cytoplasmic RNA viruses.[29] Additionally, cytoplasmic Drosha was

shown to be generated through alternative splicing and was found to cleave pri-miRNA substrates in the cytoplasm.[52,53] According to these reports, it is likely that Drosha plays a role in the processing of SeVdp vector-derived pri-miRNAs. Interestingly, the expression of cytoplasmic Drosha varies in different human cell cultures.[53] Consistent with this report, we showed that miR-124 levels differed considerably in various SeVdp-124-infected human cells (Figure 2A). Although it is unclear whether DGCR8 or other factors are responsible for miRNA processing in the cytoplasm,[29,53] our findings suggest that miRNA biogenesis in the cytoplasm may differ, in part, from that in the nucleus. We showed that SeVdp vector-derived miR-302-367 efficiently produced mature miR-367, whereas the retrovirus CX4 vector-derived miR-302-367 did not (Figure 4B). Additionally, we found that SeVdp vector-derived miR-155-based amiRNA was less effective than plasmid-derived miR-155-based amiRNA (Figures 5A; Figure S11B). These findings indicate that the unique features of miRNA transcripts may affect processing efficiency in the cytoplasm. Recent studies have suggested that sequence- and structure-dependent elements determine the affinity of pri-miRNAs for Drosha and DGCR8, as well as overall pri-miRNA processing efficiency.[38–40] Thus, it is important to investigate the mechanism underlying cytoplasmic miRNA biogenesis and determine the specific features of effective miRNA hairpins, enabling the rational design of SeVdp vectors capable of efficient small RNA production.

In summary, our findings demonstrate that the SeVdp vector enables efficient production of small regulatory RNAs. Characteristics of SeVdp vectors, such as high transduction efficiency, durable expression, and low cytotoxicity, are highly advantageous for a broad range of biological applications. Furthermore, their lack of pathogenicity to humans or risk of chromosomal insertion makes SeVdp vectors interesting tools for gene therapy, cell therapy, and regenerative medicine. These clinical applications will benefit from further improvements to the potency of SeVdp vectors.

MATERIALS AND METHODS

Plasmid Construction

To prepare psiCHECK reporter vectors for measuring miRNA activity, we inserted hybridized sense and antisense strands corresponding to the complementary sequence of the intended miRNA between the XhoI and NotI sites of the psiCHECK-2 plasmid (Promega, Madison, WI, USA). Scrambled sequences were designed using siRNA Wizard v3.1 Software (InvivoGen, San Diego, CA, USA). The DNA sequences of the miRNA targets are listed in Table S2. To prepare the psi-p53T vector, we amplified cDNA encoding the murine p53 coding sequence by PCR using the total cDNAs derived from MEFs and inserted them between AsiSI and NotI sites of the psiCHECK-2 plasmid. To prepare the pCMV-Crimson vector, we amplified cDNA encoding E2-Crimson by PCR using the pE2-Crimson Vector (Clontech, Mountain View, CA, USA) as a template, followed by incorporation into the pOL1 plasmid. To prepare the pCMV-amiFluc vectors, we prepared cDNAs encoding amiRNAs that included the complementary sequence for firefly luciferase[54] by PCR and incorporated them into the pOL1 plasmid. The sequence of the pOL1 plasmid is identical to that of pON1,[55] except for a neomycin resistance gene in place of the one for zeocin on pON1.

Cell Culture

HeLa, HeLa S3, HCT116, A549, HEK293, NHDF (KURABO, Osaka, Japan), MEF, and NIH 3T3 cells were cultured in DMEM (Sigma-Aldrich, St. Louis, MO, USA) supplemented with 10% fetal bovine serum (FBS; HyClone Laboratories, Logan, UT, USA) and penicillin-streptomycin (Pen-Strep; Wako, Osaka, Japan). Jurkat and U932 cells were cultured in RPMI 1640 (Sigma-Aldrich) supplemented with 10% FBS and Pen-Strep. Mouse iPSCs (miPSCs) were cultured in mESC medium (DMEM, 15% FBS, 0.1 mM nonessential amino acids [NEAA; Thermo Fisher Scientific, Waltham, MA, USA], 0.55 mM 2-mercaptoethanol, 1,000 U/mL leukemia inhibitory factor [LIF; Wako], and 1% Pen-Strep).

Production and Infection of SeVdp Vectors

cDNAs encoding mmu-miR-124-2 (chromosome 3 [chr3]: 17,795,418–17,796,022), mmu-miR-302-367 (chr3: 127,545,078–127,545,958), mmu-miR-9-3 (chr7: 79,505,068–79,505,570), and mmu-miR-200c (chr6: 124,718,106–124,718,583) were amplified by PCR using genomic DNA extracted from MEFs. To construct SeVdp-302-367, we mutated T and C at position 127,545,306–127,545,307 on chr3 to C and T, allowing for deletion of the EcoRI site by the QuickChange Site-Directed Mutagenesis Kit (Agilent, Santa Clara, CA, USA). cDNAs encoding EGFP, Keima-Red, and Bs^r were amplified by PCR using pEGFP-1 (Takara Bio, Kusatsu, Japan), phdKeima-Red-S1 (Medical & Biological Laboratories, Nagoya, Japan), and pCX4bsr,[56] respectively, as templates. cDNAs encoding Hyg^r, human OCT4, SOX2, and KLF4 were synthesized by GenScript (Piscataway, NJ, USA). cDNAs encoding amiRNAs that included the complementary sequence for firefly luciferase,[54] EGFP (NCBI: Pr008808666), or murine p53 (amip53#1: 5′-TGGGACAGC CAAGTCTGTTATG-3′, amip53#2: 5′-CGGGTGGAAGGAAATT TGTATC-3′) were prepared by PCR. These cDNAs were used to construct SeVdp genomic cDNAs as described previously.[33] Preparation of vector packaging cells and the production of vectors were performed as described previously.[33,55]

Cells were infected with SeVdp vectors at a MOI of 5 and incubated overnight at 37°C. The viral medium was replaced, and 10 μg/mL Bs or 100 μg/mL Hyg was added to obtain cells stably harboring the SeVdp genome.

Production and Infection of a Retroviral Vector

cDNA encoding mmu-miR-302-367 (chr3: 127,545,078–127,545,959) was inserted between the BamHI and NotI sites of pCX4pur,[56] yielding pCX4-302-367. 293T cells were transfected with pCX4-302-367, pVPack-GP (Agilent), and pVPack-Ampho (Agilent) using FuGENE HD reagent (Promega). The culture supernatant was recovered after incubation at 37°C for 3 days and then filtered through a 0.45-μm cellulose acetate filter. Viral copy number was measured using a Retroviral Titer Set (Takara Bio), and HCT116

cells were infected with 1×10^9 copies of virus supplemented with 4 μg/mL polybrene. 3 days after infection, the cells were treated with 0.2 μg/mL puromycin to select cells that stably express mmu-miR-302-367. Provirus copy number was measured based on the extracted genomic DNA using a Provirus Copy Number Detection Primer Set (Takara Bio) following the manufacturer's instructions.

Production and Infection of Lentiviral Vectors

The DNA fragment corresponding to miR-367-based amiFluc or mmu-miR-367 was inserted between the NheI and XhoI sites of pLV.SGb.PtR,[57] yielding pLV-amiFluc or pLV-367, respectively. Prodution of lentiviral vectors was performed as described previously.[57] Viral copy number was measured using a Lenti-X qRT-PCR Titration Kit (Takara Bio), and HCT116 cells were infected with LV-amiFluc or LV-367 at an MOI of 5 with 4 μg/mL polybrene. 10 days after infection, the cells were treated with 10 μg/mL Bs to select cells that stably express amiFluc or miR-367.

Generation of miPSCs

MEFs were infected with the SeVdp vector at an MOI of 3–5, followed by overnight incubation at 32°C. Next, 1.0×10^4 or 1.2×10^4 infected cells were seeded onto mitomycin C-treated MEFs in a 24-well plate and cultured in KnockOut-DMEM (Thermo Fisher Scientific) containing 15% KnockOut Serum Replacement (Thermo Fisher Scientific), 2 mM GlutaMAX (Thermo Fisher Scientific), 0.1 mM NEAA, 0.55 mM 2-mercaptoethanol, 1,000 U/mL LIF, and 1% Pen-Strep for approximately 20 days, followed by further culturing in mESC medium. To obtain transgene-free miPSCs, we transfected reprogrammed colonies with 40 nM siL527 or siP234 using Lipofectamine RNAi MAX Reagent (Thermo Fisher Scientific).[33,58] siRNA transfection was repeated four more times during subculture. siRNAs were synthesized by GeneDesign (Osaka, Japan) and Hokkaido System Science (Sapporo, Japan).

qRT-PCR

For miRNA expression analysis, total RNA was extracted using ISOGEN reagent (Nippon Gene, Tokyo, Japan), and cDNAs were synthesized using TaqMan MicroRNA Assays (Applied Biosystems, Foster City, CA, USA) and TaqMan MicroRNA Reverse Transcription Kit (Applied Biosystems). miRNA levels were determined using the TaqMan MicroRNA Assays and TaqMan Universal PCR Master Mix II, no UNG (Applied Biosystems). Total RNA of hiPSCs[55] was used as a positive control. Data was normalized to RNU48 levels. For mRNA expression analysis, total RNA was extracted using ISOGEN reagent. mESCs (EB5; RIKEN BioResource Center, Tsukuba, Japan) and miPSCs were cultured under feeder-free conditions prior to RNA extraction to avoid contamination with feeder cells. cDNAs were synthesized using the iScript gDNA Clear cDNA Synthesis Kit (Bio-Rad Laboratories, Hercules, CA, USA), and PCR was performed using SsoAdvanced Universal SYBR Green Supermix (Bio-Rad Laboratories) with primers specific to murine *p53* (forward: 5′-AAGTCCTTTGCCCTGAACTG-3′, reverse: 5′-TTTTCTTTTGC GGGGGAGAG-3′) or previously described primer sets.[8,59] Data was normalized to *GAPDH* levels.

Luciferase Assay

To determine the luciferase activity of psiCHECK vectors, we seeded 5×10^4 of SeVdp vector-infected NIH 3T3 cells or 6×10^4 of infected HCT116 cells onto a 48-well plate and transfected them with 50 ng or 25 ng of psiCHECK plasmids using Lipofectamine 2000 Reagent (Thermo Fisher Scientific), respectively. To determine the inhibitory activity of SeVdp vector- or LV vector-derived amiRNAs, we seeded 6×10^4 cells onto a 48-well plate and co-transfected them with 50 ng of the pGL3-Control vector (Promega) and 50 ng of the pRL-TK vector (Promega) using Lipofectamine 2000 reagent. To determine the activity of plasmid vector-derived amiRNAs, we seeded 6×10^4 cells onto a 48-well plate and co-transfected them with 50 ng of the amiRNA expression plasmid, 25 ng of the pGL3-Control vector, and 25 ng of the pRL-TK vector using Lipofectamine 2000. 1 day after transfection, activities of the firefly and *Renilla* luciferase were analyzed using the Dual-Luciferase Reporter Assay System (Promega) according to the manufacturer's instructions.

Fluorescence Microscopy and Image Acquisition

EGFP and E2-Crimson were detected with a fluorescence microscope (Axio Observer.A1; Zeiss, Oberkochen, Germany) using customized filters. Fluorescence was analyzed with iVision-Mac software (Solution Systems, Funabashi, Japan). Co-imaging of fluorescence for Alexa Fluor 488 (Thermo Fisher Scientific), Alexa Fluor 555 (Thermo Fisher Scientific), Alexa Fluor 647 (Thermo Fisher Scientific), and 4′,6-diamidino-2-phenylindole (DAPI) was performed using an Axio Observer or a BIOREVO BZ-9000 microscope with a BZ-II analyzer (Keyence, Osaka, Japan). To determine the activity of SeVdp vector-derived amiRNAs, we seeded 4×10^5 cells onto a 12-well plate and co-transfected with 100 ng of pEGFP-N1 (Clontech) and 100 ng of pCMV-Crimson using Lipofectamine 2000 reagent. 1 day after transfection, EGFP and E2-Crimson were detected by fluorescence microscopy.

Flow Cytometry Analysis

Briefly, 4×10^5 cells were seeded onto a 12-well plate and co-transfected with 100 ng of pEGFP-N1 and 100 ng of pCMV-Crimson using Lipofectamine 2000 reagent. 1 day after transfection, flow cytometry was performed using a Gallios flow cytometer (Beckman Coulter, Brea, CA, USA) and mean fluorescence intensity was calculated using Kaluza software (Beckman Coulter).

Immunofluorescence Staining

Cells were fixed with 3.7% formaldehyde in PBS. After permeabilization with 0.1% or 0.2% Triton X-100 in PBS, cells were incubated with a primary antibody, followed by staining with a secondary antibody conjugated to Alexa Fluor 488 (1:500), Alexa Fluor 555 (1:500), or Alexa Fluor 647 (1:500). The following primary antibodies were used, anti-SSEA1 (1:200; eBioScience, San Diego, CA, USA), anti-NANOG (1:200; Abcam, Cambridge, UK), anti-OCT4 (1:400; Abcam), anti-SOX2 (1:200; Santa Cruz Biotechnology, Dallas, TX, USA), anti-KLF4 (1:200; Santa Cruz Biotechnology), and anti-SeV-NP (1:1,000).[33] Nuclei were counterstained with DAPI using

VECTASHIELD mounting medium with DAPI (Vector Laboratories, Burlingame, CA, USA).

Statistical Analysis

The data are presented as the mean ± SD of triplicate experiments. Statistical analyses were performed using a two-tailed Student's t test.

SUPPLEMENTAL INFORMATION

Supplemental Information can be found online at https://doi.org/10.1016/j.omtm.2019.10.012.

AUTHOR CONTRIBUTIONS

M.S. conceived and designed the research. M.S., A.N., and M.O. performed the experiments. M.S., A.N., and M.O. analyzed the data. M.S. wrote the manuscript. M.S. and M.N. supervised the research. All authors reviewed and edited the manuscript.

CONFLICTS OF INTEREST

M.N. is the founder and Chief Technical Officer at TOKIWA-Bio, Inc., and this study was partly supported by a grant from TOKIWA-Bio, Inc.; however, the company had no role in study design, data collection and analysis, decision to publish, or preparation of the manuscript.

ACKNOWLEDGMENTS

We thank Dr. Makoto Miyagishi for predicting the target sites for the p53-targeted amiRNAs, Dr. Yoshio Kato for providing the plasmids for lentiviral vector production, and Dr. Minoru Iijima for technical assistance. This work was supported in part by JSPS KAKENHI (grant numbers 26750163 and 19K06501 to M.S.) and by a grant from TOKIWA-Bio, Inc.

REFERENCES

1. Carthew, R.W., and Sontheimer, E.J. (2009). Origins and Mechanisms of miRNAs and siRNAs. Cell *136*, 642–655.
2. Meister, G., and Tuschl, T. (2004). Mechanisms of gene silencing by double-stranded RNA. Nature *431*, 343–349.
3. Chakraborty, C., Sharma, A.R., Sharma, G., Doss, C.G.P., and Lee, S.S. (2017). Therapeutic miRNA and siRNA: moving from bench to clinic as next generation medicine. Mol. Ther. Nucleic Acids *8*, 132–143.
4. Bartel, D.P. (2004). MicroRNAs: genomics, biogenesis, mechanism, and function. Cell *116*, 281–297.
5. Christopher, A.F., Kaur, R.P., Kaur, G., Kaur, A., Gupta, V., and Bansal, P. (2016). MicroRNA therapeutics: Discovering novel targets and developing specific therapy. Perspect. Clin. Res. *7*, 68–74.
6. Adlakha, Y.K., and Seth, P. (2017). The expanding horizon of MicroRNAs in cellular reprogramming. Prog. Neurobiol. *148*, 21–39.
7. Sun, K., and Lai, E.C. (2013). Adult-specific functions of animal microRNAs. Nat. Rev. Genet. *14*, 535–548.
8. Anokye-Danso, F., Trivedi, C.M., Juhr, D., Gupta, M., Cui, Z., Tian, Y., Zhang, Y., Yang, W., Gruber, P.J., Epstein, J.A., and Morrisey, E.E. (2011). Highly efficient miRNA-mediated reprogramming of mouse and human somatic cells to pluripotency. Cell Stem Cell *8*, 376–388.
9. Yoo, A.S., Sun, A.X., Li, L., Shcheglovitov, A., Portmann, T., Li, Y., Lee-Messer, C., Dolmetsch, R.E., Tsien, R.W., and Crabtree, G.R. (2011). MicroRNA-mediated conversion of human fibroblasts to neurons. Nature *476*, 228–231.
10. Muraoka, N., Yamakawa, H., Miyamoto, K., Sadahiro, T., Umei, T., Isomi, M., Nakashima, H., Akiyama, M., Wada, R., Inagawa, K., et al. (2014). MiR-133 promotes cardiac reprogramming by directly repressing Snai1 and silencing fibroblast signatures. EMBO J. *33*, 1565–1581.
11. Kim, V.N., Han, J., and Siomi, M.C. (2009). Biogenesis of small RNAs in animals. Nat. Rev. Mol. Cell Biol. *10*, 126–139.
12. Iwakawa, H.O., and Tomari, Y. (2015). The functions of microRNAs: mRNA decay and translational repression. Trends Cell Biol. *25*, 651–665.
13. Zeng, Y., Yi, R., and Cullen, B.R. (2003). MicroRNAs and small interfering RNAs can inhibit mRNA expression by similar mechanisms. Proc. Natl. Acad. Sci. USA *100*, 9779–9784.
14. Silva, J.M., Li, M.Z., Chang, K., Ge, W., Golding, M.C., Rickles, R.J., Siolas, D., Hu, G., Paddison, P.J., Schlabach, M.R., et al. (2005). Second-generation shRNA libraries covering the mouse and human genomes. Nat. Genet. *37*, 1281–1288.
15. Chung, K.H., Hart, C.C., Al-Bassam, S., Avery, A., Taylor, J., Patel, P.D., Vojtek, A.B., and Turner, D.L. (2006). Polycistronic RNA polymerase II expression vectors for RNA interference based on BIC/miR-155. Nucleic Acids Res. *34*, e53.
16. Aagaard, L.A., Zhang, J., von Eije, K.J., Li, H., Saetrom, P., Amarzguioui, M., and Rossi, J.J. (2008). Engineering and optimization of the miR-106b cluster for ectopic expression of multiplexed anti-HIV RNAs. Gene Ther. *15*, 1536–1549.
17. McBride, J.L., Boudreau, R.L., Harper, S.Q., Staber, P.D., Monteys, A.M., Martins, I., Gilmore, B.L., Burstein, H., Peluso, R.W., Polisky, B., et al. (2008). Artificial miRNAs mitigate shRNA-mediated toxicity in the brain: implications for the therapeutic development of RNAi. Proc. Natl. Acad. Sci. USA *105*, 5868–5873.
18. Boudreau, R.L., Martins, I., and Davidson, B.L. (2009). Artificial microRNAs as siRNA shuttles: improved safety as compared to shRNAs in vitro and in vivo. Mol. Ther. *17*, 169–175.
19. Bauer, M., Kinkl, N., Meixner, A., Kremmer, E., Riemenschneider, M., Förstl, H., Gasser, T., and Ueffing, M. (2009). Prevention of interferon-stimulated gene expression using microRNA-designed hairpins. Gene Ther. *16*, 142–147.
20. Herrera-Carrillo, E., Liu, Y.P., and Berkhout, B. (2017). Improving miRNA delivery by optimizing miRNA expression cassettes in diverse virus vectors. Hum. Gene Ther. Methods *28*, 177–190.
21. Hacein-Bey-Abina, S., Von Kalle, C., Schmidt, M., McCormack, M.P., Wulffraat, N., Leboulch, P., Lim, A., Osborne, C.S., Pawliuk, R., Morillon, E., et al. (2003). LMO2-associated clonal T cell proliferation in two patients after gene therapy for SCID-X1. Science *302*, 415–419.
22. Hong, S., Hwang, D.Y., Yoon, S., Isacson, O., Ramezani, A., Hawley, R.G., and Kim, K.S. (2007). Functional analysis of various promoters in lentiviral vectors at different stages of in vitro differentiation of mouse embryonic stem cells. Mol. Ther. *15*, 1630–1639.
23. Norrman, K., Fischer, Y., Bonnamy, B., Wolfhagen Sand, F., Ravassard, P., and Semb, H. (2010). Quantitative comparison of constitutive promoters in human ES cells. PLoS ONE *5*, e12413.
24. Rouha, H., Thurner, C., and Mandl, C.W. (2010). Functional microRNA generated from a cytoplasmic RNA virus. Nucleic Acids Res. *38*, 8328–8337.
25. Shapiro, J.S., Varble, A., Pham, A.M., and tenOever, B.R. (2010). Noncanonical cytoplasmic processing of viral microRNAs. RNA *16*, 2068–2074.
26. Varble, A., Chua, M.A., Perez, J.T., Manicassamy, B., García-Sastre, A., and tenOever, B.R. (2010). Engineered RNA viral synthesis of microRNAs. Proc. Natl. Acad. Sci. USA *107*, 11519–11524.
27. Langlois, R.A., Shapiro, J.S., Pham, A.M., and tenOever, B.R. (2012). In vivo delivery of cytoplasmic RNA virus-derived miRNAs. Mol. Ther. *20*, 367–375.
28. Honda, T., Yamamoto, Y., Daito, T., Matsumoto, Y., Makino, A., and Tomonaga, K. (2016). Long-term expression of miRNA for RNA interference using a novel vector system based on a negative-strand RNA virus. Sci. Rep. *6*, 26154.
29. Shapiro, J.S., Langlois, R.A., Pham, A.M., and tenOever, B.R. (2012). Evidence for a cytoplasmic microprocessor of pri-miRNAs. RNA *18*, 1338–1346.
30. Usme-Ciro, J.A., Campillo-Pedroza, N., Almazán, F., and Gallego-Gomez, J.C. (2013). Cytoplasmic RNA viruses as potential vehicles for the delivery of therapeutic small RNAs. Virol. J. *10*, 185.

31. Jaenisch, R., and Young, R. (2008). Stem cells, the molecular circuitry of pluripotency and nuclear reprogramming. Cell *132*, 567–582.

32. Nakanishi, M., and Otsu, M. (2012). Development of Sendai virus vectors and their potential applications in gene therapy and regenerative medicine. Curr. Gene Ther. *12*, 410–416.

33. Nishimura, K., Sano, M., Ohtaka, M., Furuta, B., Umemura, Y., Nakajima, Y., Ikehara, Y., Kobayashi, T., Segawa, H., Takayasu, S., et al. (2011). Development of defective and persistent Sendai virus vector: a unique gene delivery/expression system ideal for cell reprogramming. J. Biol. Chem. *286*, 4760–4771.

34. Suh, M.R., Lee, Y., Kim, J.Y., Kim, S.K., Moon, S.H., Lee, J.Y., Cha, K.Y., Chung, H.M., Yoon, H.S., Moon, S.Y., et al. (2004). Human embryonic stem cells express a unique set of microRNAs. Dev. Biol. *270*, 488–498.

35. Liao, B., Bao, X., Liu, L., Feng, S., Zovoilis, A., Liu, W., Xue, Y., Cai, J., Guo, X., Qin, B., et al. (2011). MicroRNA cluster 302-367 enhances somatic cell reprogramming by accelerating a mesenchymal-to-epithelial transition. J. Biol. Chem. *286*, 17359–17364.

36. Subramanyam, D., Lamouille, S., Judson, R.L., Liu, J.Y., Bucay, N., Derynck, R., and Blelloch, R. (2011). Multiple targets of miR-302 and miR-372 promote reprogramming of human fibroblasts to induced pluripotent stem cells. Nat. Biotechnol. *29*, 443–448.

37. Wang, G., Guo, X., Hong, W., Liu, Q., Wei, T., Lu, C., Gao, L., Ye, D., Zhou, Y., Chen, J., et al. (2013). Critical regulation of miR-200/ZEB2 pathway in Oct4/Sox2-induced mesenchymal-to-epithelial transition and induced pluripotent stem cell generation. Proc. Natl. Acad. Sci. USA *110*, 2858–2863.

38. Zhang, X., and Zeng, Y. (2010). The terminal loop region controls microRNA processing by Drosha and Dicer. Nucleic Acids Res. *38*, 7689–7697.

39. Auyeung, V.C., Ulitsky, I., McGeary, S.E., and Bartel, D.P. (2013). Beyond secondary structure: primary-sequence determinants license pri-miRNA hairpins for processing. Cell *152*, 844–858.

40. Nguyen, T.A., Jo, M.H., Choi, Y.G., Park, J., Kwon, S.C., Hohng, S., Kim, V.N., and Woo, J.S. (2015). Functional anatomy of the human microprocessor. Cell *161*, 1374–1387.

41. Wilson, K.D., Venkatasubrahmanyam, S., Jia, F., Sun, N., Butte, A.J., and Wu, J.C. (2009). MicroRNA profiling of human-induced pluripotent stem cells. Stem Cells Dev. *18*, 749–758.

42. Zuker, M. (2003). Mfold web server for nucleic acid folding and hybridization prediction. Nucleic Acids Res. *31*, 3406–3415.

43. Varble, A., Benitez, A.A., Schmid, S., Sachs, D., Shim, J.V., Rodriguez-Barrueco, R., Panis, M., Crumiller, M., Silva, J.M., Sachidanandam, R., and tenOever, B.R. (2013). An in vivo RNAi screening approach to identify host determinants of virus replication. Cell Host Microbe *14*, 346–356.

44. Takayama, K., Morisaki, Y., Kuno, S., Nagamoto, Y., Harada, K., Furukawa, N., Ohtaka, M., Nishimura, K., Imagawa, K., Sakurai, F., et al. (2014). Prediction of interindividual differences in hepatic functions and drug sensitivity by using human iPS-derived hepatocytes. Proc. Natl. Acad. Sci. USA *111*, 16772–16777.

45. Nishimura, T., Kaneko, S., Kawana-Tachikawa, A., Tajima, Y., Goto, H., Zhu, D., Nakayama-Hosoya, K., Iriguchi, S., Uemura, Y., Shimizu, T., et al. (2013). Generation of rejuvenated antigen-specific T cells by reprogramming to pluripotency and redifferentiation. Cell Stem Cell *12*, 114–126.

46. Wakao, H., Yoshikiyo, K., Koshimizu, U., Furukawa, T., Enomoto, K., Matsunaga, T., Tanaka, T., Yasutomi, Y., Yamada, T., Minakami, H., et al. (2013). Expansion of functional human mucosal-associated invariant T cells via reprogramming to pluripotency and redifferentiation. Cell Stem Cell *12*, 546–558.

47. Nakagawa, M., Koyanagi, M., Tanabe, K., Takahashi, K., Ichisaka, T., Aoi, T., Okita, K., Mochiduki, Y., Takizawa, N., and Yamanaka, S. (2008). Generation of induced pluripotent stem cells without Myc from mouse and human fibroblasts. Nat. Biotechnol. *26*, 101–106.

48. Miyoshi, N., Ishii, H., Nagano, H., Haraguchi, N., Dewi, D.L., Kano, Y., Nishikawa, S., Tanemura, M., Mimori, K., Tanaka, F., et al. (2011). Reprogramming of mouse and human cells to pluripotency using mature microRNAs. Cell Stem Cell *8*, 633–638.

49. Amarzguioui, M., Rossi, J.J., and Kim, D. (2005). Approaches for chemically synthesized siRNA and vector-mediated RNAi. FEBS Lett. *579*, 5974–5981.

50. Grimm, D., Streetz, K.L., Jopling, C.L., Storm, T.A., Pandey, K., Davis, C.R., Marion, P., Salazar, F., and Kay, M.A. (2006). Fatality in mice due to oversaturation of cellular microRNA/short hairpin RNA pathways. Nature *441*, 537–541.

51. Miyoshi, K., Miyoshi, T., and Siomi, H. (2010). Many ways to generate microRNA-like small RNAs: non-canonical pathways for microRNA production. Mol. Genet. Genomics *284*, 95–103.

52. Dai, L., Chen, K., Youngren, B., Kulina, J., Yang, A., Guo, Z., Li, J., Yu, P., and Gu, S. (2016). Cytoplasmic Drosha activity generated by alternative splicing. Nucleic Acids Res. *44*, 10454–10466.

53. Link, S., Grund, S.E., and Diederichs, S. (2016). Alternative splicing affects the subcellular localization of Drosha. Nucleic Acids Res. *44*, 5330–5343.

54. Elbashir, S.M., Harborth, J., Lendeckel, W., Yalcin, A., Weber, K., and Tuschl, T. (2001). Duplexes of 21-nucleotide RNAs mediate RNA interference in cultured mammalian cells. Nature *411*, 494–498.

55. Sano, M., Iijima, M., Ohtaka, M., and Nakanishi, M. (2016). Novel strategy to control transgene expression mediated by a Sendai virus-based vector using a nonstructural C protein and endogenous microRNAs. PLoS ONE *11*, e0164720.

56. Akagi, T., Sasai, K., and Hanafusa, H. (2003). Refractory nature of normal human diploid fibroblasts with respect to oncogene-mediated transformation. Proc. Natl. Acad. Sci. USA *100*, 13567–13572.

57. Kato, Y., Sawata, S.Y., and Inoue, A. (2010). A lentiviral vector encoding two fluorescent proteins enables imaging of adenoviral infection via adenovirus-encoded miRNAs in single living cells. J. Biochem. *147*, 63–71.

58. Sano, M., Ohtaka, M., Iijima, M., Nakasu, A., Kato, Y., and Nakanishi, M. (2017). Sensitive and long-term monitoring of intracellular microRNAs using a non-integrating cytoplasmic RNA vector. Sci. Rep. *7*, 12673.

59. Stadtfeld, M., Apostolou, E., Akutsu, H., Fukuda, A., Follett, P., Natesan, S., Kono, T., Shioda, T., and Hochedlinger, K. (2010). Aberrant silencing of imprinted genes on chromosome 12qF1 in mouse induced pluripotent stem cells. Nature *465*, 175–181.